Atmos. Chem. Phys. Discuss., https://doi.org/10.5194/acp-2018-1159
Manuscript under review for journal Atmos. Chem. Phys.
Discussion started: 21 December 2018

Atmospheric Chemistry and Physics
Discussions
Open Access

Arctic cloud annual cycle biases in climate models

Patrick C. Taylor[1], Robyn C. Boeke[2], Ying Li[3] and David W.J. Thompson[3]

[1]NASA Langley Research Center, Climate Science Branch, Hampton, Virginia, USA
[2]Science Systems Applications Inc., Hampton, Virginia, USA
[3]Colorado State University, Department of Atmospheric Science, Fort Collins, Colorado, USA

Correspondence to: Patrick C. Taylor (Patrick.c.taylor@nasa.gov)

Abstract. Arctic clouds exhibit a robust annual cycle with maximum cloudiness in fall and minimum in winter. These variations affect energy flows in the Arctic with a large influence on the surface radiative fluxes. Contemporary climate models struggle to reproduce the observed Arctic cloud amount annual cycle and significantly disagree with each other. The goal of this analysis is to quantify the cloud influencing factors that contribute to winter-summer cloud amount differences, as these seasons are primarily responsible for the model discrepancies with observations. We find that differences in the total cloud amount annual cycle are primarily caused by differences in low, not high, clouds; the largest differences occur between the surface and 950 hPa. Stratifying cloud amount by cloud influencing factors, we find that model groups disagree most under strong lower tropospheric stability, weak to moderate mid-tropospheric subsidence, and cold lower tropospheric air temperatures. Inter-group differences in low cloud amount are found to be a function of the dependence of low cloud amount on the lower tropospheric thermodynamic characteristics. We find that models with a larger low cloud amount in winter produce more cloud ice, whereas models with a larger low cloud amount in summer produce more cloud liquid. Thus, the parameterization of ice microphysics, specifically the ice formation mechanism (deposition vs. immersion freezing) and cloud liquid and ice partitioning, contributes to the inter-model differences in the Arctic cloud annual cycle and provides further evidence of the important role that cloud ice microphysical processes play in the evolution and modeling of the Arctic climate system.

1. Introduction

Arctic clouds, arguably one of the most poorly understood aspects of the Arctic climate system, strongly modulate radiative energy fluxes at the surface, through the atmosphere, and to the top of the atmosphere (Cesana et al., 2012; Curry et al., 1996; Kay et al., 2008; Kay & L'Ecuyer, 2013; Shupe & Intrieri, 2004). As such, Arctic clouds have the potential to influence climate variability and change in the Arctic and globally. For instance, the presence of clouds in winter over sea ice can be the difference between a -40 W m^{-2} surface radiative energy imbalance and a balanced surface radiation budget, influencing surface temperature and sea ice growth rate (H. Morrison et al., 2012; Persson et al., 2002, 2017). Accurately representing clouds in climate models is therefore necessary to realistically simulate the evolution of the Arctic surface energy budget.

Contemporary climate models, however, strongly disagree with observations on the seasonality of Arctic cloud radiative effects. Observations indicate that Arctic clouds cool the surface through the reflection of solar radiation for a few months during summer and warm the surface through enhanced downwelling longwave radiation the rest of the year (Kay & L'Ecuyer, 2013; Shupe & Intrieri, 2004). Climate models possess significant biases in the seasonality of the surface cloud radiative effect (Boeke & Taylor, 2016; Karlsson & Svensson, 2013; Karlsson & Svensson, 2011). Climate models participating in the Coupled Model Intercomparison Project 5 (CMIP5) (Taylor et al., 2011) simulate Arctic clouds that are too reflective in summer and not insulating enough in winter. These cloud radiative effect biases trace to a number of errors in cloud properties: namely, insufficient Arctic cloud amount (English et al., 2015), inaccurate partitioning of cloud water between the liquid and ice phase leading to excessive ice clouds (Cesana et al., 2012; Kay et al., 2016) and insufficient supercooled liquid clouds (Komurcu et al., 2014). This study focuses on errors in model-simulated Arctic cloud amount and its annual cycle.

Arctic cloud amount exhibits a robust annual cycle that has been known for some time (Hahn et al., 1995; Huschke, 1969). However, important revisions to our understanding of the cloud amount annual cycle have occurred since the launch of the CloudSat Cloud Profiling Radar (Stephens et al., 2008) and the Cloud-Aerosol Lidar with Orthogonal Polarization (CALIOP) (Winker et al., 2010). As illustrated in Liu et al., (2012), both ground observer and satellite passive radiometer retrieval data sets indicate a broad summer maximum in cloud amount extending into September, declining through fall, and reaching an annual cycle minimum in winter. Both data sets suffer from the lack of sunlight in fall and winter. Passive cloud retrieval algorithms also change with surface type, posing additional challenges (Minnis et al., 2011). CALIOP and CloudSAT active remote sensing instruments provide cloud amount data independent of surface type with high accuracy in the absence of sunlight. Active remote sensing observations indicate that average Arctic cloud amount exceeds 65% for each month reaching ~90% in fall (Boeke & Taylor, 2016; Liu et al., 2012) and that previous data sets missed ~10-15% of fall cloud cover. Space-based active retrievals are not without limitations, most important of which is a 25-40% under detection of clouds below 500 meters relative to surface-based remote sensing observations (Liu et al., 2017). However, CALIOP and CloudSAT cloud amount data still provide the most complete characterization of vertically-resolved Arctic-wide cloud amount.

Despite the refined observational knowledge of the Arctic cloud annual cycle, the mechanisms that control it remain an open question. Beesley & Moritz (1999) outline several physical controls on Arctic clouds including surface-atmosphere coupling, large-scale meteorology, and cloud microphysics. The surface-atmospheric coupling mechanism implies—less sea ice, more surface evaporation—that Arctic cloud amount should follow the annual cycle of sea ice. Observationally, this mechanism has been shown to operate under specific conditions in fall, whereby reduced sea ice cover corresponds to increased cloud amount, but not in summer (Kay & Gettelman, 2009; Morrison et al., 2018; Taylor et al., 2015). Second, seasonal changes in large-scale meteorology, atmospheric advection, and humidity influence the cloud amount annual cycle. Previous work demonstrates a significant dependence of cloud properties on local atmospheric conditions (Barton et al., 2012; Kay & Gettelman, 2009; Li et al., 2014; Liu & Schweiger, 2017). Lower tropospheric stability has a profound influence on Arctic low cloud amount, whereby increased stability corresponds to reduced cloud amount (Taylor et al., 2015). Third, cloud microphysical processes affect cloud amount and exhibit a seasonality tied to temperature, whereby colder temperatures support ice crystal formation and precipitation (Beesley & Moritz, 1999). In addition, the seasonality of aerosol amount and composition can influence cloud amount and properties by altering microphysics (Coopman et al., 2018; Jackson et al., 2012).

Atmos. Chem. Phys. Discuss., https://doi.org/10.5194/acp-2018-1159
Manuscript under review for journal Atmos. Chem. Phys.
Discussion started: 21 December 2018

Atmospheric Chemistry and Physics Discussions

Given the lack of mechanistic understanding of the drivers of the Arctic cloud annual cycle, it comes as no surprise that climate models struggle to simulate the Arctic cloud amount annual cycle. Comparison of the CALIOP-CloudSAT total column cloud amount with CMIP5 models indicates that individual models differ from observations by more than 15% in summer and 40% in winter (Boeke & Taylor, 2016). Further, Boeke & Taylor, (2016) show that several models produce peak cloud cover in winter with others producing peak cloud cover in summer; few models capture the observed fall cloud cover peak. Thus, the majority of models misrepresent the annual cycle of Arctic cloud cover. Meteorological reanalysis data products are not immune and also exhibit similar errors in the Arctic cloud amount annual cycle timing (Liu & Key, 2016).

The combination of poor model simulation and the lack of mechanistic understanding of the drivers of the Arctic cloud annual cycle signals a critical gap in our understanding with significant consequences for our ability to attribute, simulate, and predict Arctic climate variability and change. We address this gap by investigating the drivers of the inter-model differences in the Arctic cloud annual cycle in CMIP5 climate models. As previous studies indicate, Arctic cloud amount is influenced by its environment; a fact that guides this analysis. We adopt a methodology stratifying climate model simulated vertically-resolved cloud amount by several key cloud influencing factors, described in Section 2. The stratification methodology, discussed in Section 3, enables us to explore the dependence of simulated cloud amount on individual and groups of cloud influencing factors and how they differ across the CMIP5 models. In section 4, our key results are compared with previous work (Li et al., 2014) and our understanding of the mechanisms driving the Arctic cloud annual cycle is discussed. Lastly, Section 5 highlights the insights gained into how the Arctic cloud annual cycle influences Arctic climate variability and change and our ability to simulate it.

2. Methodology and Models

The goal of this analysis is to explain the divergent representations of the Arctic cloud amount annual cycle found in contemporary climate models. We use the historical forcing simulations (prescribed greenhouse gases and land use changes consistent with observations from 1979-2005) from 24 CMIP5 climate models (Taylor et al., 2011) with the available output in the archive (https://esgf-node.llnl.gov/projects/cmip5/). Monthly mean variables used include vertically-resolved cloud amount, air temperature (T_A), relative humidity (*RH*), 500 hPa vertical velocity (ω_{500}), sensible heat flux (*SHF*), latent heat flux (*LHF*), liquid and ice water mixing ratios (*CLW* and *CLI*, respectively), sea ice concentration (*SIC*) and lower tropospheric stability (*LTS*). Lower tropospheric stability is defined as the potential temperature difference between the surface and 700 hPa, computed from the monthly-averaged temperature profile.

Several observed and reanalysis variables are included as a reference to gauge the fidelity of the model results. The Modern-Era Retrospective Analysis for Research and Applications-2 (MERRA-2) provides information on the Arctic atmospheric conditions. MERRA-2 has a horizontal resolution of 0.5° latitude x 0.625° longitude and vertical resolution of 72 hybrid-eta levels fully described in Molod et al., (2015). The observed vertically-resolved Arctic cloud amount are derived from CALIPSO-CloudSAT-CERES-MODIS (C3M) data (Kato et al., 2010).

The primary methodology composites cloud amount into bins of individual cloud influencing factors, adapted from Li et al., (2014). The cloud influencing factors considered include ω_{500}, *LTS*, *SHF*, *LHF*, *SIC*, and vertically-resolved T_A and *RH*. The primary difference between the present analysis and Li et al., (2014) is the use of monthly-averaged model output instead of instantaneous satellite data. We also extend our analysis beyond single variables and construct joint distributions.

Lastly, the results are composited and analyzed within two groups based upon key features of the simulated Arctic total cloud amount annual cycle. Figure 1a shows that the cloud amount annual cycles from individual models tend to follow one of two patterns: one showing the largest cloud amount in winter and small seasonal variations, and another showing minimum cloud amount in winter, peak summertime cloud amount, and large seasonal amplitude. Figure 2 summarizes these two patterns showing a scatterplot of the average winter (DJF) and summer (JJA) cloud amounts for individual models motivating the separation of the 24 models into two groups; models that simulate a larger total cloud amount in winter are referred to as Group 1 (10 models) and models that simulate a larger total cloud amount in summer are referred to as Group 2 (14 models). While the models can be grouped in several different ways, the choice to delineate model groups above and below the diagonal 1:1 line in Fig. 2 clearly places models with similar cloud amount annual cycle shapes together while also grouping them based on how they differ from observations. Group 1 models fail to reproduce the correct timing of the maximum cloud amount, showing peak cloud amount in winter while C3M shows minimum cloud amount in winter. Group 2 models correctly simulate the season of minimum cloud amount (winter), but possess a much larger-amplitude annual cycle than C3M and a summer peak in cloud amount as opposed to fall. This separation is also motivated by the need to understand the factors (e.g., microphysics, surface turbulent fluxes, dynamics, and thermodynamics) responsible for producing clouds in these individual seasons to provide insight as to the cause(s) of Arctic cloud amount annual cycle differences between models. The application of this grouping allows us to consolidate the analysis and take a deeper look at the influencing factors.

3. Results

3.1. Vertical variations of the cloud amount annual cycle

Figure 3 illustrates the vertically-resolved average cloud amount annual cycle for each group. Group 1 (Fig. 3a) exhibits a minimum in low cloud amount (>850 hPa) in May through July with maximum low cloud amount in January and February. Group 1 high cloud amount follows a similar seasonal pattern as low clouds with a minimum in summer and maximum in the fall/winter at reduced amplitude. Group 2 (Fig. 3b) exhibits a similar high cloud amount annual cycle as Group 1 with smaller cloud amounts and a weaker amplitude. However, the annual cycle of low cloud indicates that cloud amount slowly increases in amount and extends in height through summer, then sharply decreases after September, in sharp contrast with observations and Group 1 (Fig. 3f,g). The standard deviation in cloud amount across each group (Fig. 3d,e) indicates that the largest intra-group differences occur at vertical levels and times of year with the largest cloud amount, below 800 hPa and above 500 hPa in winter for both groups and below 800 hPa in summer. The only exception is in Group 1 where larger standard deviations occur in summer below 800 hPa, when Group 1 models show minimum cloud amount.

Figure 1b,c illustrates the inter-model difference in the seasonal cycle of Arctic cloud amount for low clouds (1000-850 hPa) and high clouds (500-300 hPa), respectively. The results in Figs. 1b,c demonstrate that low clouds predominantly contribute to the winter versus summer peaks in the simulated seasonal cycle of the total cloud amount. The rest of this paper analyzes how the dependence of cloud amount on the cloud influencing factors contributes to these differences in Arctic low cloud amount in winter versus summer. The goal of this paper is to understand how, why, and to what extent do the cloud influencing factors contribute to the differences in the Arctic low cloud amount with winter peaks in Group 1 and summer peaks in Group 2.

3.2. Horizontal variation in the cloud amount annual cycle

The above differences in the annual cycle of the Arctic clouds between Groups 1 and 2 are based on the averages over the entire Arctic region, in this subsection we further confirm that such differences are spatially uniform. Figure 4 illustrates the spatial variations of the low and high cloud amount differences for Group 1 minus Group 2. In winter, Group 1 produces an average of 12.4% more low clouds than Group 2 (Fig. 4a) and 7.3% fewer low clouds in summer (Fig. 4c). These differences are generally spatially uniform. Differences in high cloud amount show similar spatial uniformity but with Group 1 producing more high clouds than Group 2 in both winter (+6.4%) and summer (+3.7%) (Fig. 4b,c). These differences show weak spatial variability and thus indicate that regional differences do not significantly contribute to the annual cycle differences in low or high cloud amount.

Since atmospheric and surface properties vary across the Arctic and can influence the simulated cloud amount, we also analyze the spatial variations in the cloud influencing factors for the model groups (not shown) finding that the differences between Group 1 and 2 exhibit a general spatial uniformity with only minor deviations. As such, the following stratification analysis is performed over the entire Arctic region

.

3.3. Inter-group differences in mean and distribution of atmospheric conditions

Arctic cloud formation is influenced by a number of atmospheric characteristics including surface and boundary layer thermodynamic properties and large-scale dynamics (Kay & Gettelman, 2009; Z. Liu & Schweiger, 2017; Taylor et al., 2015). Table 1 and Figure 5 provide the annual-mean ensemble averages of cloud influencing factors for each group and their probability density function (PDF) over the ocean and land surfaces. The average properties in Table 1 for the two groups are generally similar. A difference of means tests between the groups show statistically significant differences for all cloud influencing factors at 95% confidence. Intergroup differences for most cloud influencing factors, however, are small suggesting that differences in the average atmospheric conditions do not drive intergroup differences in the cloud amount annual cycle. Notable exceptions are *RH* and *CLW* over both surface types. Group 2 possesses higher *RH* values and almost twice the average *CLW* of Group 1. Overall, the spread in the average cloud influencing factors is larger within each group than between Group 1 and 2.

The variability of individual cloud influencing factors is consistent between the groups with some small differences. The PDFs in Fig. 5 summarize the frequency of the cloud influencing factors for Group 1 (red) and Group

2 (blue) separated into land (cross-hatching) and ocean (solid). Figure 5 includes PDFs of each variable derived from MERRA-2 reanalysis and shown in solid black lines for ocean (square symbols) and land (triangle symbols). In most cases, the distribution of cloud influencing factors is similar between the two groups for each surface type. The most notable differences are (1) Group 2 models exhibit a higher frequency of stronger *LTS* values for both land and ocean (Fig. 5a) and (2) Group 2 $-\omega_{500}$ exhibits a higher frequency of values near 0 hPa day^{-1} over both land and ocean (Fig. 5b). In these cases, Group 1 $-\omega_{500}$ over land and ocean and *LTS* over ocean is more consistent with MERRA-2. Additional group differences are seen in *RH* (Fig. 5g), *CLI* (Fig. 5d) and *CLW* (Fig. 5h) whereby Group 2 favors higher *RH* and larger *CLW* while Group 1 shows a larger *CLI* and a higher frequency of *CLW* values near 0 g kg^{-1}.

3.4. Dependence of vertically-resolved cloud amount on cloud influencing factors

We investigate the possibility that intergroup differences in cloud amount are explained by differences in the relationship between cloud amount and cloud influencing factors. Figure 6 shows the vertically-resolved average cloud amount binned by five different cloud influencing factors ($-\omega_{500}$, *LTS*, ice water path (*IWP*), total condensed water path (*CLWVI*; ice plus liquid water path), and *SIC*. Since Group 1 shows a winter cloud amount peak in the annual cycle, it is expected that Group 1 produces larger cloud amounts than Group 2 throughout the troposphere and especially below 850 hPa for most cloud influencing factors (Fig. 6, right column). Figure 6a,b illustrates the cloud vertical structure as a function of $-\omega_{500}$ and reveals a general increase in cloud amount as the strength of rising motion increases at most levels for both groups over ocean (from left to right in Fig. 6a,b) and land (Fig. S1). Group 1 exhibits a deviation from this behavior at pressures >950 hPa showing almost no dependence on $-\omega_{500}$; cloud amount is large under both sinking and rising motion. The inter-group differences (Fig. 6c) indicate that Group 1 produces larger cloud amount than Group 2 throughout the troposphere and particularly at pressures >950 hPa.

Figure 6d,e illustrates a similar dependence of the vertically-resolved average cloud amount stratified by *LTS*. Both groups exhibit a general decrease in cloud amount with stronger *LTS* at all levels and over both ocean and land (Fig. S1); in other words, as conditions become more stable clouds tend to occur in a shallower layer closer to the surface, also found in observations (Taylor et al., 2015). Much like $-\omega_{500}$, Group 1 produces equal or larger cloud amounts at pressures >950 hPa as *LTS* increases, signaling a potentially important $-\omega_{500}$-*LTS* covariance. Specifically, the average cloud amount is >20% larger in Group 1 than in Group 2 when *LTS* > 20 K at pressures >950 hPa. The larger cloud amount at pressures >950 hPa can be viewed as either a difference in a dissipative mechanism (e.g., turbulent mixing, cloud microphysics, or precipitation) between the groups or a difference in cloud production (e.g., ice formation or surface-driven buoyancy).

Figure 6g,h,j,k illustrates the dependence of cloud amount on *IWP* and *CLWVI*. Models in both groups favor more cloud amount with higher cloud bases for increasing *IWP* and *CLWVI*; both surface types exhibit similar behavior. Group 1 diverges from Group 2 at lower values of *IWP* and *CLWVI* (< ~35 g m^{-2}) by producing maximum cloud amount in the thin cloud regime at pressures >950 hPa (Fig. 6g,j) while Group 2 shows minimum cloud amount. For the average wintertime values of *IWP* (~32 g m^{-2}) and *CLWVI* (~52 g m^{-2}), Group 1 has larger cloud amount than Group 2 at all levels over ocean and land.

The influence of surface conditions on cloud amount over the Arctic Ocean is assessed using *SIC*. Representing an integral measure of the surface influence on cloud amount, increased *SIC* generally corresponds to decreases in surface turbulent fluxes and stronger *LTS* (Pavelsky et al., 2011; Taylor et al., 2018). Figure 6m,n illustrates that both groups produce a decrease in cloud amount and lower cloud bases with increased *SIC*; the cloud amount decrease is muted in Group 1 compared to Group 2 (Fig. 6o) as with *LTS*. However, the inter-group differences at high *SIC* values are smaller than for *LTS* (Fig. 6f,o). Overall, the inter-group differences illustrate a weak dependence on *SIC* in winter.

Figure 7 shows the vertically-resolved average cloud amount dependence on five different cloud influencing factors ($-\omega_{500}$, *LTS*, *IWP*, *CLWVI*, and *SIC*) over land (excluding *SIC*, which is over ocean) for summer (JJA). Since Group 2 models possess a summer cloud amount peak (especially for low clouds), it is expected that Group 2 models generally produce larger cloud amount than Group 1 throughout the troposphere for almost all cloud influencing factors (right column). We show results over land in summer because differences exceed 20% over land and are 5-10% over ocean. The largest inter-group differences are again at pressures >950 hPa, in this case Group 2 exhibits larger cloud amount than Group 1. Important findings from Fig. 7 include (1) the inter-group differences in cloud amount are ~5-10% smaller during summer, (2) Group 2 tends to produce more clouds at pressures >950 hPa for all cloud influencing factors, (3) all dependencies of cloud amount on cloud influencing factors are weaker than in winter, and (4) neither group exhibits a dependence of the average cloud fraction on *SIC*.

The winter and summer analyses reveal several key takeaways. First, the primary intergroup differences are found at pressures >950 hPa in the thin low cloud regime. Second, the differences in the cloud amount dependence on cloud influencing factors are larger during winter than summer. Third, the largest inter-group differences in winter are found under stable conditions and sinking motion and in summer under rising motion. The fact that intergroup differences in the cloud amount dependence are largest for *LTS* and $-\omega_{500}$ and the expectation of significant covariances between these two variables warrants a joint distribution analysis to address the question, why are Group 1 models able to maintain large low cloud amount under strong stability and subsidence?

3.5. Joint PDFs: *LTS* and $-\omega_{500}$

Figure 8 shows the joint distribution of average low cloud amount stratified by both *LTS* and $-\omega_{500}$ (Fig. 8a-b) with the corresponding frequency of occurrence of each bin in winter contoured over top for Group 1 (Fig. 8a) and Group 2 (Fig. 8b). Cloud amount depends on (1) the relationship between the cloud amount and *LTS* and $-\omega_{500}$ and (2) how frequently each LTS and $-\omega_{500}$ bin occurs. For regions with *LTS*<12 K, low cloud amount for both groups is primarily a function of *LTS* with little dependence on $-\omega_{500}$; the intergroup differences illustrate the same behavior (Fig. 8c). Considering *LTS* >12 K, low cloud amount exhibits a dependence on both *LTS* and $-\omega_{500}$, however the intergroup differences still correspond with only to variations in *LTS*.

While both groups simulate the highest frequency of occurrence of $-\omega_{500}$ bin around -4 hPa day^{-1}, Group 1 most frequently simulates *LTS* values between 22-24 K whereas Group 2 simulates higher values between 26-30 K (Fig. 8a,b, contours). Thus, the inter-group difference is marked by a dipole pattern along the LTS axis between 22-24 K and 26-30 K, and these regions primarily contribute to the winter low cloud amount between Group 1 and Group 2.

Figure 9 shows the joint distribution of low cloud amount by *LTS* and $-\omega_{500}$ bins in summer. The pattern in the summer low cloud amount (Fig. 9a,b) is more similar between the groups than in winter yielding smaller inter-group differences (Fig. 9c). Considering *LTS*<14 K, low cloud amount depends primarily on *LTS* with a weak dependence on $-\omega_{500}$. For *LTS*>14 K however, low cloud amount depends on both *LTS* and $-\omega_{500}$, a behavior similar to winter. Figure 9a,b illustrates that the low cloud amount gradients are sharper in summer than winter, meaning that summer low cloud amount is more susceptible to small changes in *LTS* and $-\omega_{500}$ than in winter. The inter-group differences in frequency of occurrence indicates that Group 2 exhibits higher *LTS* values (20-25 K) and lower *LTS* values (<12 K) more frequently.

The winter or summer average low cloud amount can be estimated from the terms illustrated in Figs. 8 and 9 using

$$\overline{LCA} = \sum_{i,j} LCA\left(LTS_i, -\omega_{500,j}\right) * RFO\left(LTS_i, -\omega_{500,j}\right). \quad (1)$$

This expression describes the weighted sum of the low cloud amount over all LTS_i and $-\omega_{500,j}$ from each i, j bin, where $LCA\left(LTS_i, -\omega_{500,j}\right)$ corresponds to the low cloud amount as a function of LTS_i and $-\omega_{500,j}$ and $RFO\left(LTS_i, -\omega_{500,j}\right)$ corresponds to the relative frequency of occurrence of each LTS_i and $-\omega_{500,j}$ bin. Applying (1) to compute the average low cloud amount, $\overline{LCA}$, in either winter or summer reproduces the winter and summer average low cloud amount for each group to within 1-2% percent (Table 2). We construct $LCA\left(LTS_i, -\omega_{500,j}\right)$ by averaging, which removes some variability. As such, eq. (1) parameterizes low cloud amount and is not expected to exactly reproduce $\overline{LCA}$. This exercise indicates that $\overline{LCA}$ can be accurately reconstructed using the $LCA\left(LTS_i, -\omega_{500,j}\right)$ and $RFO\left(LTS_i, -\omega_{500,j}\right)$ suggesting that this approach is applicable in interpreting drivers of interannual variability or feedbacks in low cloud amount.

Equation (1) can be applied to both Group 1 and Group 2, and then the inter-group differences (Group 1 minus Group 2; $\overline{\delta LCA_{G1-G2}}$) can be estimated and decomposed using a first-order Taylor series approximation to further quantify the relative contributions from differences in 1) $\delta LCA\left(LTS_i, -\omega_{500,j}\right)$ and 2) $\delta RFO\left(LTS_i, -\omega_{500,j}\right)$.

$$\overline{\delta LCA_{G1-G2}} = \sum_{i,j}\left[\left(\delta LCA\left(LTS_i, -\omega_{500,j}\right)_{G1-G2} * RFO\left(LTS_i, -\omega_{500,j}\right)_{G1}\right)\right] +$$
$$\sum_{i,j}\left[\left(LCA\left(LTS_i, -\omega_{500,j}\right)_{G1} * \delta RFO\left(LTS_i, -\omega_{500,j}\right)_{G1-G2}\right)\right] \quad (2)$$

In (2), $\overline{\delta LCA_{G1-G2}}$ corresponds to the inter-group difference (Group 1 minus Group 2) in average low cloud amount, $\delta LCA\left(LTS_i, -\omega_{500,j}\right)_{G1-G2}$ corresponds to the inter-group difference in the dependence of low cloud amount on *LTS* and $-\omega_{500}$ dependence, and $\delta RFO\left(LTS_i, -\omega_{500,j}\right)_{G1-G2}$ corresponds to the inter-group difference in the relative frequency of occurrence of *LTS* and $-\omega_{500}$ bins. In this framework, the first term on the right-hand side, $\delta LCA\left(LTS_i, -\omega_{500,j}\right)_{G1-G2}$, represents the influence of the parameterized cloud physics and the second term, $\delta RFO\left(LTS_i, -\omega_{500,j}\right)_{G1-G2}$, represents the influence of atmospheric state occurrence. Table 3 summarizes the results and overwhelmingly indicates that the $\delta LCA\left(LTS_i, -\omega_{500,j}\right)_{G1-G2}$ term is responsible for the summer and winter inter-group differences in low cloud amount.

While this result attributes the Group 1 minus Group 2 differences to parameterized cloud physics and not the atmospheric state occurrence, it does not explain the fundamental cause. The cause(s) is due to differences in the specifics of the parameterized cloud physics, systematic differences in the atmospheric conditions grouped by *LTS* and $-\omega_{500}$ bins, or a combination of both. A systematic exploration of the intergroup differences in cloud physics parameterizations are beyond the scope of this study. We explore the intergroup differences in atmospheric conditions within *LTS* and $-\omega_{500}$ bins to assess their influence on low cloud amount differences.

Characterizing atmospheric state by *LTS* and $-\omega_{500}$ bins does not account for all inter-group differences in atmospheric state. Thus, we consider atmospheric and surface conditions stratified by *LTS* and $-\omega_{500}$. Both groups exhibit similar distributions of lower tropospheric *RH*, 950-hPa T_A, *SHF*, *LHF*, and *SIC* (not shown) within the *LTS* and $-\omega_{500}$ bins in winter (Fig. 10) and summer (Fig. S3). Inter-group differences in *RH* (Fig. 10c) are generally <5% and anti-correlate with intergroup low cloud amount differences; in other words, Group 2 exhibits smaller low cloud amount than Group 1 and yet has a larger *RH*, more frequently simulating values >80% (Fig. 5g). Alternatively, Group 1 is colder than Group 2 in the most frequently occurring bins (Fig. 10f) and this could lead to differences in cloud microphysics and ice formation. Inter-model differences in *SHF* and *LHF* indicate that the intergroup differences change sign with increasing *LTS*; however, these differences anti-correlate with the intergroup differences in low cloud amount.

Intergroup differences in cloud microphysics and specifically the production of cloud liquid versus ice strongly corresponds to intergroup differences in low cloud amount. Figure 11 illustrates the differences in lower tropospheric *CLW* and *CLI* stratified by *LTS* and $-\omega_{500}$. Both groups exhibit similar overall dependencies of the liquid and ice water mixing ratio on *LTS* and $-\omega_{500}$. Intergroup differences clearly show that Group 2 models produce more cloud liquid whereas Group 1 models produce more ice; Fig. 12 illustrates that same results in summer. Figures 11 and 12 support our idea that Group 1 models sustain a larger production of cloud ice at cold temperatures supporting larger low cloud amount in winter. Moreover, the finding that Group 1 models are drier than Group 2 suggests that the enhanced cloud ice formation dehydrates the winter Arctic atmosphere in these models. The smaller *CLW* in Group 1 is also related to the greater *CLI* as some models do not allow supersaturation with respect to ice meaning that liquid supersaturation would not be reached under most Arctic winter conditions. Alternatively, the larger cloud liquid production by Group 2 corresponds to a larger low cloud amount in summer. The correspondence between larger production of cloud liquid and larger low cloud fraction in summer is due to warmer temperatures being less favorable for cloud ice formation. The results support the argument that cloud phase partitioning and cloud microphysical parameterizations explain the differences in the Arctic cloud amount annual cycle and differences in the surface turbulent fluxes and atmospheric circulation contribute little. Therefore, improved representation of the Arctic cloud amount annual cycle requires improvements in the representation of cloud microphysical processes in thin, low clouds.

Due to the importance of T_A and *RH* to this explanation, we further investigate the low cloud amount dependence on T_A and *RH* as both variables influence the cloud microphysical parameterizations. Figures 13 and 14 illustrate the joint distribution of the average low cloud amount stratified by lower tropospheric T_A and *RH* and the frequency of occurrence of each bin in winter and summer, respectively. The largest intergroup differences are found at the coldest temperatures and highest *RH* values for both winter (Fig. 13) and summer (Fig. 14). Group 1 favors cooler and drier atmospheric conditions than Group 2 (Fig. 13c), while also producing more clouds under those conditions. In summer, Group 2 models produce larger low cloud amounts compared to Group 1 in the warmer and more humid conditions that occur most frequently (Fig. 14). Group 2 also slightly favors more humid conditions in summer than Group 1 contributing to larger summer low cloud amount. Results applying the decomposition from (1) to the T_s and RH joint distribution indicate that winter differences in the parameterized cloud physics are primarily responsible for δLCA_{G1-G2}, where as in summer the relative frequency of occurrence is primarily responsible for δLCA_{G1-G2} (Table 3). This result supports our conclusion that cloud microphysical processes explain the model differences in Arctic low cloud amount in winter. In summer, however, Fig. 14 indicates that processes that control the frequency of occurrence of T_s and RH states are also important to explain low cloud amount differences.

4. Discussion

This analysis explores the factors that influence Arctic cloud amount within contemporary climate models with the specific focus on understanding the factors that drive differences in the Arctic cloud amount annual cycle. In comparing our results with previous work, the vertically-resolved cloud amount dependencies (Figs. 6 and 7) on cloud influencing factors agrees with the observationally-based analysis of Li et al., (2014). It should be noted that this result is despite differences in the temporal characteristics of the two analyses: monthly-averaged model output vs. instantaneous satellite data. This result implies that the use of monthly averages is not as big of a limiting factor for investigating the cloud dependence on atmospheric and surface conditions as previously assumed. Our results demonstrate that climate model physical parameterizations realistically reproduce the general Arctic cloud amount dependence on atmospheric conditions, yet subtle differences produce large differences in the Arctic cloud amount annual cycle.

We argue that the primary cause of the larger cloud amount in Group 1 during winter is due to the production and maintenance of low clouds at colder surface air temperatures than Group 2. We hypothesize that Group 1 maintains low cloud amount at colder temperatures as a result of ice microphysical parameterization differences by producing more cloud ice than Group 2 overall and especially at colder temperatures and lower RH. This hypothesis seems at odds with previous cloud process research considering the mixed-phase cloud system where cloud ice production desiccates super cooled liquid and more efficiently precipitates reducing low cloud amount (Avramov et al., 2011; Morrison et al., 2012). In this case, the results suggest that Group 1 overcomes this by producing more cloud ice. Our result does not imply that this process relationship between cloud ice production and super cooled liquid does not operate in climate models, as we cannot assess the frequency of mixed-phase clouds using monthly averaged output. Overall, the importance of cloud microphysics to model cloud amounts is consistent with previous work illustrating that Arctic clouds and their radiative effects strongly respond to changes in ice microphysics (English et al., 2014; Kay et al., 2016; McCoy et al., 2016; Tan & Storelvmo, 2015).

What do our results argue about the drivers of the Arctic cloud annual cycle? The climate model results argue that the Arctic cloud annual cycle is most strongly driven by the seasonality of cloud microphysics, specifically the cloud phase and temperature relationship. The *SIC* in both the inter-group differences as well as the cloud amount dependence on *SIC* shows a weaker relationship than the other factors indicating a limited role in driving the Arctic cloud annual cycle. The results also do not support a significant role for the seasonality of *RH* in forcing the Arctic low cloud annual cycle because (1) the seasonality of *RH* is similar between the two groups (Fig. S3) and (2) models that produce fewer winter clouds possess higher *RH*. Rather, the cloud microphysics appear to shape Arctic lower tropospheric *RH*. Changes in atmospheric conditions, specifically *LTS* and $-\omega_{500}$, are significant between winter and summer indicating a role for the large-scale circulation. Our results support the idea of Beesley & Moritz (1999) that the covariance between atmospheric temperature and cloud microphysics is a major factor responsible for the Arctic cloud annual cycle.

The cloud ice formation process becomes a critical consideration. Models that do not allow supersaturation with respect to ice implicitly assume that deposition freezing is the dominant ice formation process in Arctic low clouds. However, observational evidence indicates that supercooled liquid must first be present before cloud ice is observed at temperatures warmer than -25°C, supporting the notion that immersion freezing is the dominant process (de Boer et al., 2011). Our results indicate that a better understanding of ice formation mechanisms operating in the Arctic and the conditions under which each dominates would provide an important constraint on climate model physics and Arctic climate simulations.

A new idea from this analysis is one of Arctic cloud susceptibility. Returning to the *LTS* and $-\omega_{500}$ joint distributions, summer versus winter differences (Figs. 8a,b, and 9a,b) in the low cloud amount dependence are significant. Figures 8 and 9 show that the most frequently occurring atmospheric conditions in summer are found along a strong gradient in the low cloud amount dependence on *LTS* and $-\omega_{500}$, not the case for winter. This suggests that summer low cloud amount is more susceptible to changes in atmospheric conditions than winter low clouds. This apparent difference in the susceptibility of low cloud amount to changes in atmospheric conditions could have important implications for Arctic cloud feedback, as (Taylor, 2016) illustrates that changes in *LTS* imply large changes in the surface cloud radiative effect.

5. Conclusion

Surface and space-based observations of Arctic clouds exhibit a robust annual cycle with maximum cloud amount in fall and a minimum in winter. Variations in cloud amount affect energy flows in the Arctic and strongly influence the surface energy budget. Therefore, understanding the role of clouds in the context of the present-day Arctic climate is imperative for improving predictions of surface temperature and sea ice variability, as well as for projecting Arctic climate change. As we and several authors before demonstrate, contemporary climate models struggle to reproduce observed Arctic cloud amount and its variability, especially within the context of the annual cycle.

Our analysis focuses on identifying the causes of the climate model differences in the annual cycle representation. We find that most climate models tend to fall into one of two groups: one favoring larger winter cloud amount and another favoring larger summer cloud amount. The results demonstrate that differences in low, thin clouds at pressures >950 hPa, not middle or high clouds, are primarily responsible for the total cloud amount annual cycles within each group. These discrepancies between the two model groups exhibit little spatial variability, are consistent between land

Atmos. Chem. Phys. Discuss., https://doi.org/10.5194/acp-2018-1159
Manuscript under review for journal Atmos. Chem. Phys.
Discussion started: 21 December 2018

Atmospheric Chemistry and Physics
Open Access
Discussions

and ocean, and are only weakly influenced by sea ice concentration, suggesting that the cause of the cloud amount differences operates Arctic-wide.

Differences in atmospheric and surface conditions represent an important potential source of the low cloud amount differences. The results show small differences in the annual, domain-averaged atmospheric and surface conditions between the two groups and indicate that these are not responsible for the low cloud amount differences. Considering specific atmospheric and surface conditions, we find that models disagree most under strong lower tropospheric stability, weak to moderate mid-tropospheric subsidence, and cold lower tropospheric air temperatures. Overall, the cloud amount dependence on cloud influencing factors explains most of the inter-group differences in cloud amount. Since, the cloud amount dependence on cloud influencing factors in climate models is governed by parameterized cloud physics, the results indicate that parameterization differences are responsible for the cloud amount discrepancies and that differences in the frequency of occurrence of atmospheric and surface conditions between the models is not a significant factor.

Why do models simulate different low cloud amounts under specific atmospheric conditions? Models produce similar dependencies of low cloud amount on atmospheric and surface conditions in summer but not in winter. Models able to sustain larger low cloud amounts at colder surface air temperatures simulate more winter clouds and we argue that the details of the ice microphysical parameterization are responsible by causing a larger production of cloud ice in some models than others. The present analysis is unable to isolate the specific characteristics of the ice microphysical parameterization (e.g., ice formation, crystal habit, mass-diameter relationship, fall speed, gamma size distribution parameters, etc.) that drive these differences, however this should be the focus of future investigation. A commonality of these ice microphysical parameterization characteristics is that few observational constraints are available.

Our results have several implications to our understanding and modeling of Arctic climate.

- Cloud ice microphysical processes are important contributors to the Arctic low cloud amount annual cycle and therefore are important to the seasonality of the Arctic surface energy budget and sea ice cover.
- Mean Arctic low cloud amount is strongly constrained by atmospheric variability, namely by the lower tropospheric stability and mid-tropospheric vertical motion fields.
- Lower tropospheric stability plays an important role in explaining the inter-model differences in low cloud amount.
- Cloud microphysical parameterizations drive significant inter-model differences in Arctic cloud amount and its annual cycle.
- Improved modeling of the Arctic cloud amount annual cycle, and its influences on Arctic climate variability and change, requires observational constraints on ice microphysical processes, particularly on cloud phase partitioning and ice formation mechanisms.
- The general thinking that models producing too much ice then desiccate supercooled liquid and yield fewer clouds does not explain model biases in low cloud amount. Our results indicate that in winter larger ice production supports larger low cloud amounts, likely because models simulate very little supercooled liquid in winter. Larger supercooled liquid water is associated with larger low cloud amounts in summer.

In closing, Arctic cloud amount plays a significant role in shaping Arctic climate system evolution. Given the stark evidence that the Arctic climate is changing more rapidly than the rest of the globe, improved modeling capabilities in this highly varying, highly susceptible, and geopolitically important region is urgent. A better understanding of Arctic clouds is vital to providing this improved capability. This analysis advances our understanding of the factors that drive Arctic cloud behavior in climate models and points to unresolved issues in ice microphysics as the likely explanation. Thus, our results underscore the vital need for observational constraints on these critical processes.

Code availability: Computer code used for the analysis was written in IDL and is available from the authors upon request.

Author Contributions: PCT and RCB formulated the studied, performed the analysis, and PCT, RCM, YL, and DWJT

Competing Interests: The authors declare no competing interests.

Data Availability: The CMIP5 model data analyzed and supports the finding of this study are deposited in the Earth System Grid Federation Peer-to-Peer enterprise system and available at https://esgf-node.llnl.gov/projects/esgf-llnl/.

Acknowledgements: This work is funded by the NASA Program grant number NNH16ZDA001N-NDOA. We acknowledge the World Climate Research Programme's Working Group on Coupled Modelling, which is responsible for CMIP. For CMIP the U.S. Department of Energy's Program for Climate Model Diagnosis and Intercomparison provides coordinating support and leads development of software infrastructure in partnership with the Global Organization for Earth System Science Portals.

References

Avramov, A., Ackerman, A. S., Fridlind, A. M., Diedenhoven, B. van, Botta, G., Aydin, K., et al. (2011). Toward ice formation closure in Arctic mixed-phase boundary layer clouds during ISDAC. *Journal of Geophysical Research: Atmospheres*, *116*(D1). https://doi.org/10.1029/2011JD015910

Barton, N. P., Klein, S. A., Boyle, J. S., & Zhang, Y. Y. (2012). Arctic synoptic regimes: Comparing domain-wide Arctic cloud observations with CAM4 and CAM5 during similar dynamics. *Journal of Geophysical Research: Atmospheres (1984–2012)*, *117*(D15). https://doi.org/10.1029/2012JD017589

Beesley, J. A., & Moritz, R. E. (1999). Toward an Explanation of the Annual Cycle of Cloudiness over the Arctic Ocean. *Journal of Climate*, *12*(2), 395–415. https://doi.org/10.1175/1520-0442(1999)012<0395:TAEOTA>2.0.CO;2

Boeke, R. C., & Taylor, P. C. (2016). Evaluation of the Arctic surface radiation budget in CMIP5 models. *Journal of Geophysical Research: Atmospheres*, *121*(14), 2016JD025099. https://doi.org/10.1002/2016JD025099

Boer, G. de, Morrison, H., Shupe, M. D., & Hildner, R. (2011). Evidence of liquid dependent ice nucleation in high-latitude stratiform clouds from surface remote sensors. *Geophysical Research Letters*, *38*(1). https://doi.org/10.1029/2010GL046016

Cesana, G., Kay, J. E., Chepfer, H., English, J. M., & de Boer, G. (2012). Ubiquitous low-level liquid-containing Arctic clouds: New observations and climate model constraints from CALIPSO-GOCCP. *Geophysical Research Letters*, *39*(20), L20804. https://doi.org/10.1029/2012GL053385

Coopman, Q., Garrett, T. J., Finch, D. P., & Riedi, J. (2018). High Sensitivity of Arctic Liquid Clouds to Long-Range Anthropogenic Aerosol Transport. *Geophysical Research Letters*, *45*(1), 372–381. https://doi.org/10.1002/2017GL075795

Curry, J. A., Schramm, J. L., Rossow, W. B., & Randall, D. (1996). Overview of Arctic Cloud and Radiation Characteristics. *Journal of Climate*, *9*(8), 1731–1764. https://doi.org/10.1175/1520-0442(1996)009<1731:OOACAR>2.0.CO;2

English, J. M., Kay, J. E., Gettelman, A., Liu, X., Wang, Y., Zhang, Y., & Chepfer, H. (2014). Contributions of Clouds, Surface Albedos, and Mixed-Phase Ice Nucleation Schemes to Arctic Radiation Biases in CAM5. *Journal of Climate*, *27*(13), 5174–5197. https://doi.org/10.1175/JCLI-D-13-00608.1

English, J. M., Gettelman, A., & Henderson, G. R. (2015). Arctic Radiative Fluxes: Present-Day Biases and Future Projections in CMIP5 Models. *Journal of Climate*, *28*(15), 6019–6038. https://doi.org/10.1175/JCLI-D-14-00801.1

Hahn, C. J., Warren, S. G., & London, J. (1995). The Effect of Moonlight on Observation of Cloud Cover at Night, and Application to Cloud Climatology. *Journal of Climate*, *8*(5), 1429–1446. https://doi.org/10.1175/1520-0442(1995)008<1429:TEOMOO>2.0.CO;2

Huschke, R. E. (1969). *ARCTIC CLOUD STATISTICS FROM "AIR-CALIBRATED" SURFACE WEATHER OBSERVATIONS*, (No. RM-6173-PR). RAND CORP SANTA MONICA CALIF. Retrieved from http://www.dtic.mil/docs/citations/AD0698740

Jackson, R. C., McFarquhar, G. M., Korolev, A. V., Earle, M. E., Liu, P. S. K., Lawson, R. P., et al. (2012). The dependence of ice microphysics on aerosol concentration in arctic mixed-phase stratus clouds during ISDAC and M-PACE. *Journal of Geophysical Research: Atmospheres*, *117*(D15). https://doi.org/10.1029/2012JD017668

Karlsson, J., & Svensson, G. (2013). Consequences of poor representation of Arctic sea-ice albedo and cloud-radiation interactions in the CMIP5 model ensemble. *Geophysical Research Letters*, *40*(16), 4374–4379. https://doi.org/10.1002/grl.50768

Karlsson, Johannes, & Svensson, G. (2011). The simulation of Arctic clouds and their influence on the winter surface temperature in present-day climate in the CMIP3 multi-model dataset. *Climate Dynamics*, *36*(3), 623–635. https://doi.org/10.1007/s00382-010-0758-6

Kato, S., Sun-Mack, S., Miller, W. F., Rose, F. G., Chen, Y., Minnis, P., & Wielicki, B. A. (2010). Relationships among cloud occurrence frequency, overlap, and effective thickness derived from CALIPSO and CloudSat merged cloud vertical profiles. *Journal of Geophysical Research: Atmospheres*, *115*(D4). https://doi.org/10.1029/2009JD012277

Kay, J. E., & Gettelman, A. (2009). Cloud influence on and response to seasonal Arctic sea ice loss. *Journal of Geophysical Research: Atmospheres*, *114*(D18), D18204. https://doi.org/10.1029/2009JD011773

Kay, J. E., & L'Ecuyer, T. (2013). Observational constraints on Arctic Ocean clouds and radiative fluxes during the early 21st century. *Journal of Geophysical Research: Atmospheres*, *118*(13), 7219–7236. https://doi.org/10.1002/jgrd.50489

Kay, J. E., L'Ecuyer, T., Gettelman, A., Stephens, G., & O'Dell, C. (2008). The contribution of cloud and radiation anomalies to the 2007 Arctic sea ice extent minimum. *Geophysical Research Letters*, *35*(8), L08503. https://doi.org/10.1029/2008GL033451

Kay, J. E., L'Ecuyer, T., Chepfer, H., Loeb, N., Morrison, A., & Cesana, G. (2016). Recent Advances in Arctic Cloud and Climate Research. *Current Climate Change Reports*, *2*(4), 159–169. https://doi.org/10.1007/s40641-016-0051-9

Komurcu, M., Storelvmo, T., Tan, I., Lohmann, U., Yun, Y., Penner, J. E., et al. (2014). Intercomparison of the cloud water phase among global climate models. *Journal of Geophysical Research: Atmospheres*, *119*(6), 3372–3400. https://doi.org/10.1002/2013JD021119

Li, Y., Thompson, D. W. J., Stephens, G. L., & Bony, S. (2014). A global survey of the instantaneous linkages between cloud vertical structure and large-scale climate. *Journal of Geophysical Research: Atmospheres*, *119*(7), 3770–3792. https://doi.org/10.1002/2013JD020669

Li, Y., Thompson, D. W. J., Huang, Y., & Zhang, M. (2014). Observed linkages between the northern annular mode/North Atlantic Oscillation, cloud incidence, and cloud radiative forcing. *Geophysical Research Letters*, *41*(5), 1681–1688. https://doi.org/10.1002/2013GL059113

Liu, Y., & Key, J. R. (2016). Assessment of Arctic Cloud Cover Anomalies in Atmospheric Reanalysis Products Using Satellite Data. *Journal of Climate*, *29*(17), 6065–6083. https://doi.org/10.1175/JCLI-D-15-0861.1

Liu, Y., Key, J. R., Ackerman, S. A., Mace, G. G., & Zhang, Q. (2012). Arctic cloud macrophysical characteristics from CloudSat and CALIPSO. *Remote Sensing of Environment*, *124*, 159–173. https://doi.org/10.1016/j.rse.2012.05.006

Liu, Y., Shupe, M. D., Wang, Z., & Mace, G. (2017). Cloud vertical distribution from combined surface and space radar–lidar observations at two Arctic atmospheric observatories. *Atmospheric Chemistry and Physics*, *17*(9), 5973–5989. https://doi.org/10.5194/acp-17-5973-2017

Liu, Z., & Schweiger, A. (2017). Synoptic Conditions, Clouds, and Sea Ice Melt Onset in the Beaufort and Chukchi Seasonal Ice Zone. *Journal of Climate*, *30*(17), 6999–7016. https://doi.org/10.1175/JCLI-D-16-0887.1

McCoy, D. T., Tan, I., Hartmann, D. L., Zelinka, M. D., & Storelvmo, T. (2016). On the relationships among cloud cover, mixed-phase partitioning, and planetary albedo in GCMs. *Journal of Advances in Modeling Earth Systems*, *8*(2), 650–668. https://doi.org/10.1002/2015MS000589

Minnis, P., Sun-Mack, S., Young, D. F., Heck, P. W., Garber, D. P., Chen, Y., et al. (2011). CERES Edition-2 Cloud Property Retrievals Using TRMM VIRS and Terra and Aqua MODIS Data—Part I: Algorithms. *IEEE Transactions on Geoscience and Remote Sensing*, *49*(11), 4374–4400. https://doi.org/10.1109/TGRS.2011.2144601

Molod, A., Takacs, L., Suarez, M., & Bacmeister, J. (2015). Development of the GEOS-5 atmospheric general circulation model: evolution from MERRA to MERRA2. *Geoscientific Model Development*, *8*(5), 1339–1356. https://doi.org/10.5194/gmd-8-1339-2015

Morrison, A. L., Kay, J. E., Chepfer, H., Guzman, R., & Yettella, V. (2018). Isolating the Liquid Cloud Response to Recent Arctic Sea Ice Variability Using Spaceborne Lidar Observations. *Journal of Geophysical Research: Atmospheres*, *123*(1), 473–490. https://doi.org/10.1002/2017JD027248

Morrison, H., de Boer, G., Feingold, G., Harrington, J., Shupe, M. D., & Sulia, K. (2012). Resilience of persistent Arctic mixed-phase clouds. *Nature Geoscience*, *5*(1), 11–17. https://doi.org/10.1038/ngeo1332

Pavelsky, T. M., Boé, J., Hall, A., & Fetzer, E. J. (2011). Atmospheric inversion strength over polar oceans in winter regulated by sea ice. *Climate Dynamics*, *36*(5–6), 945–955. https://doi.org/10.1007/s00382-010-0756-8

Persson, P. O. G., Fairall, C. W., Andreas, E. L., Guest, P. S., & Perovich, D. K. (2002). Measurements near the Atmospheric Surface Flux Group tower at SHEBA: Near-surface conditions and surface energy budget. *Journal of Geophysical Research: Oceans*, *107*(C10), 8045. https://doi.org/10.1029/2000JC000705

Persson, P. O. G., Shupe, M. D., Perovich, D., & Solomon, A. (2017). Linking atmospheric synoptic transport, cloud phase, surface energy fluxes, and sea-ice growth: observations of midwinter SHEBA conditions. *Climate Dynamics*, *49*(4), 1341–1364. https://doi.org/10.1007/s00382-016-3383-1

Shupe, M. D., & Intrieri, J. M. (2004). Cloud Radiative Forcing of the Arctic Surface: The Influence of Cloud Properties, Surface Albedo, and Solar Zenith Angle. *Journal of Climate*, *17*(3), 616–628. https://doi.org/10.1175/1520-0442(2004)017<0616:CRFOTA>2.0.CO;2

Stephens, G. L., Vane, D. G., Tanelli, S., Im, E., Durden, S., Rokey, M., et al. (2008). CloudSat mission: Performance and early science after the first year of operation. *Journal of Geophysical Research: Atmospheres*, *113*(D8). https://doi.org/10.1029/2008JD009982

Tan, I., & Storelvmo, T. (2015). Sensitivity Study on the Influence of Cloud Microphysical Parameters on Mixed-Phase Cloud Thermodynamic Phase Partitioning in CAM5. *Journal of the Atmospheric Sciences*, *73*(2), 709–728. https://doi.org/10.1175/JAS-D-15-0152.1

Taylor, K. E., Stouffer, R. J., & Meehl, G. A. (2011). An Overview of CMIP5 and the Experiment Design. *Bulletin of the American Meteorological Society*, *93*(4), 485–498. https://doi.org/10.1175/BAMS-D-11-00094.1

Taylor, P., Hegyi, B., Boeke, R., Boisvert, L., Taylor, P. C., Hegyi, B. M., et al. (2018). On the Increasing Importance of Air-Sea Exchanges in a Thawing Arctic: A Review. *Atmosphere*, *9*(2), 41. https://doi.org/10.3390/atmos9020041

Taylor, P. C. (2016). Does a relationship between Arctic low clouds and sea ice matter? In *AIP Conference Proceedings* (Vol. 1810). American Institue of Physics. http://dx.doi.org/10.1063/1.4975520

Taylor, P. C., Kato, S., Xu, K.-M., & Cai, M. (2015). Covariance between Arctic sea ice and clouds within atmospheric state regimes at the satellite footprint level. *Journal of Geophysical Research: Atmospheres*, *120*(24), 12656–12678. https://doi.org/10.1002/2015JD023520

Winker, D. M., Pelon, J., Coakley, J. A., Ackerman, S. A., Charlson, R. J., Colarco, P. R., et al. (2010). The CALIPSO Mission. *Bulletin of the American Meteorological Society*, *91*(9), 1211–1230. https://doi.org/10.1175/2010BAMS3009.1

Table 1: Annual mean atmospheric conditions for MERRA-2, Group 1, Group 2 for ocean and land, and the 95% confidence interval for the difference in means (Group 1 – Group 2).

OCEAN

	MERRA-2	GROUP 1	GROUP 2	95% CI OF $\mu_{G1} - \mu_{G2}$
LTS (K)	21.29	20.67	22.30	$-1.64 < \mu_{G1}-\mu_{G2} < -1.62$
$-\omega_{500}$ (hPa day^{-1})	-1.67	0.90	-0.33	$1.20 < \mu_{G1}-\mu_{G2} < 1.25$
SHF (W m^{-2})	8.69	4.55	6.66	$-2.15 < \mu_{G1}-\mu_{G2} < -2.08$
LHF (W m^{-2})	12.56	11.85	11.74	$0.07736 < \mu_{G1}-\mu_{G2} < 0.151$
LOW CLOUD (%)	25.10	25.60	21.74	$3.86 < \mu_{G1}-\mu_{G2} < 3.88$
HIGH CLOUD (%)	16.50	18.00	12.84	$5.16 < \mu_{G1}-\mu_{G2} < 5.18$
SIC (%)		73.68	73.00	$0.616 < \mu_{G1}-\mu_{G2} < 0.742$
LOW-LEVEL RH (%)	83.40	79.50	84.10	$-4.61 < \mu_{G1}-\mu_{G2} < -4.59$
LOW-LEVEL T_A (K)	262.00	260.90	261.40	$-0.50 < \mu_{G1}-\mu_{G2} < -0.46$
CLI (g kg^{-1})	0.0016	0.0050	0.0040	$0.0010 < \mu_{G1}-\mu_{G2} < 0.00101$
CLW (g kg^{-1})	0.0180	0.0140	0.0240	$-0.010 < \mu_{G1}-\mu_{G2} < -0.010$

LAND

	MERRA-2	GROUP 1	GROUP 2	95% CI OF $\mu_{G1} - \mu_{G2}$
LTS (K)	19.69	19.91	19.87	$0.022 < \mu_{G1}-\mu_{G2} < 0.05$
$-\omega_{500}$ (hPa day^{-1})	1.35	-3.73	-0.48	$-3.31 < \mu_{G1}-\mu_{G2} < -3.12$
SHF (W m^{-2})	7.31	0.74	1.51	$-0.821 < \mu_{G1}-\mu_{G2} < -0.714$
LHF (W m^{-2})	22.96	15.32	13.11	$2.17 < \mu_{G1}-\mu_{G2} < 2.25$
LOW CLOUD (%)	19.80	22.67	19.63	$3.02 < \mu_{G1}-\mu_{G2} < 3.05$
HIGH CLOUD (%)	17.5	21.15	15.33	$5.80 < \mu_{G1}-\mu_{G2} < 5.82$
LOW-LEVEL RH (%)	82.00	77.00	81.80	$-4.80 < \mu_{G1}-\mu_{G2} < -4.78$
LOW-LEVEL T_A (K)	266.00	263.30	264.10	$-0.83 < \mu_{G1}-\mu_{G2} < -0.78$
CLI (g kg^{-1})	0.0009	0.0045	0.0041	$0.00039 < \mu_{G1}-\mu_{G2} < 0.0004$
CLW (g kg^{-1})	0.0200	0.0160	0.0260	$-0.0094 < \mu_{G1}-\mu_{G2} < -0.0093$

Atmos. Chem. Phys. Discuss., https://doi.org/10.5194/acp-2018-1159
Manuscript under review for journal Atmos. Chem. Phys.
Discussion started: 21 December 2018

Table 2: Summary of the average low cloud amount for each group from model output and as computed using Equation (1).

	GROUP 1	GROUP 2
DJF domain-averaged LCA	29.0%	17.2%
DJF LCA from Eq. (1)	29.8%	16.3%
JJA domain-averaged LCA	23.1%	27.0%
JJA LCA from Eq. (1)	21.8%	26.1%

Table 3: Summary of decomposition results attributing Group 1 minus Group 2 differences in the average low cloud amount following Equation (2).

AVERAGE LCA CONSTRUCTED FROM [LTS_i, $-\omega_{500,j}$]

	$\overline{\Delta LCA}_{G1-G2}$	$\overline{\delta LCA}_{G1-G2}$	$\delta LCA_{G1-G2} \cdot RFO_{G1}$	$LCA_{G1} \cdot \delta RFO_{G1-G2}$
WINTER	11.80%	13.30%	13.10%	0.17%
SUMMER	-3.84%	-4.45%	-4.49%	0.05%

AVERAGE LCA CONSTRUCTED FROM [$T_{a,i}$, RH_j]

	$\overline{\Delta LCA}_{G1-G2}$	$\overline{\delta LCA}_{G1-G2}$	$\delta LCA_{G1-G2} \cdot RFO_{G1}$	$LCA_{G1} \cdot \delta RFO_{G1-G2}$
WINTER	11.60%	10.40%	12.20%	-1.80%
SUMMER	-4.20%	-4.68%	-1.37%	-3.31%

Atmos. Chem. Phys. Discuss., https://doi.org/10.5194/acp-2018-1159
Manuscript under review for journal Atmos. Chem. Phys.
Discussion started: 21 December 2018

Atmospheric Chemistry and Physics
Open Access
Discussions

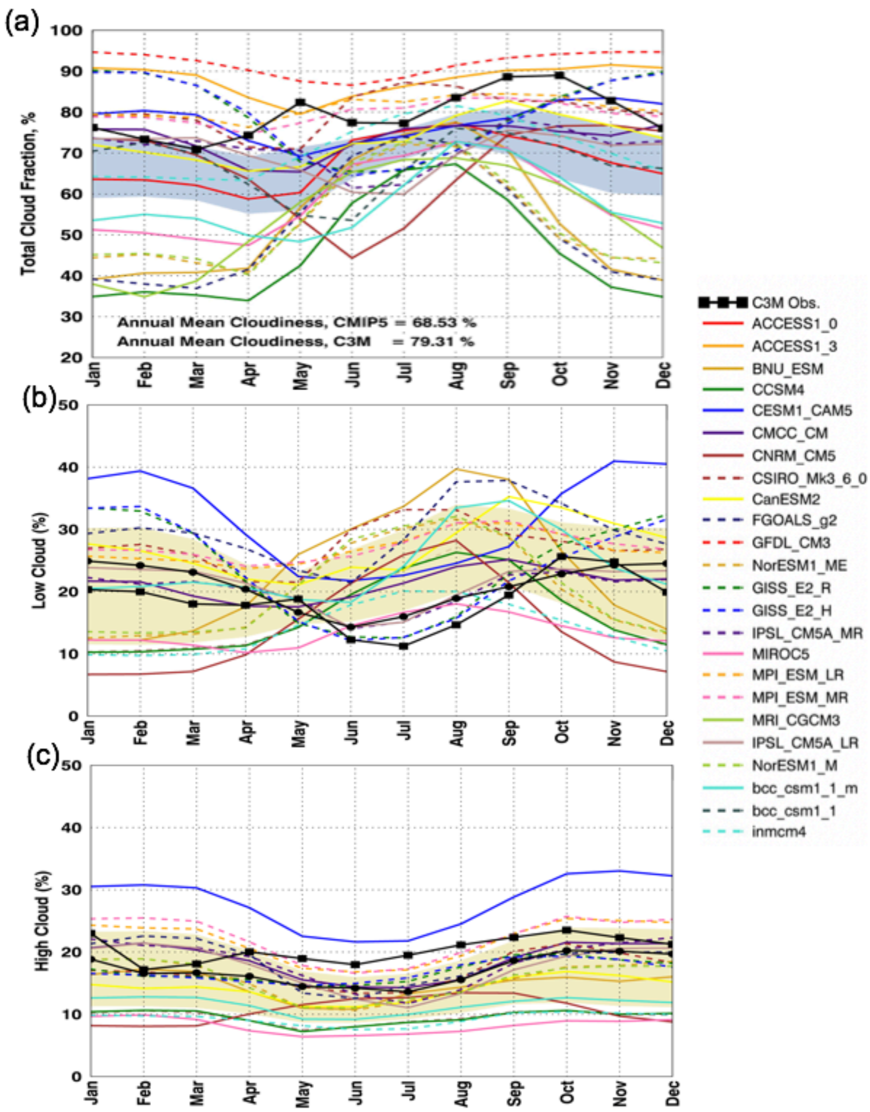

Figure 1: Annual cycle of (a) total cloud amount, (b) low cloud amount (defined as cloud between 1000 – 850 hPa) and (c) high cloud amount (cloud between 500 – 300 hPa). Color lines represent individual CMIP5 models. The black line with squares represents C3M observations and the black line with circles represents MERRA-2. The gray shading in (a) represents the 95% confidence interval for the difference in means between C3M and the ensemble; the yellow shading in (b)-(c) represents the ensemble mean +/- one standard deviation.

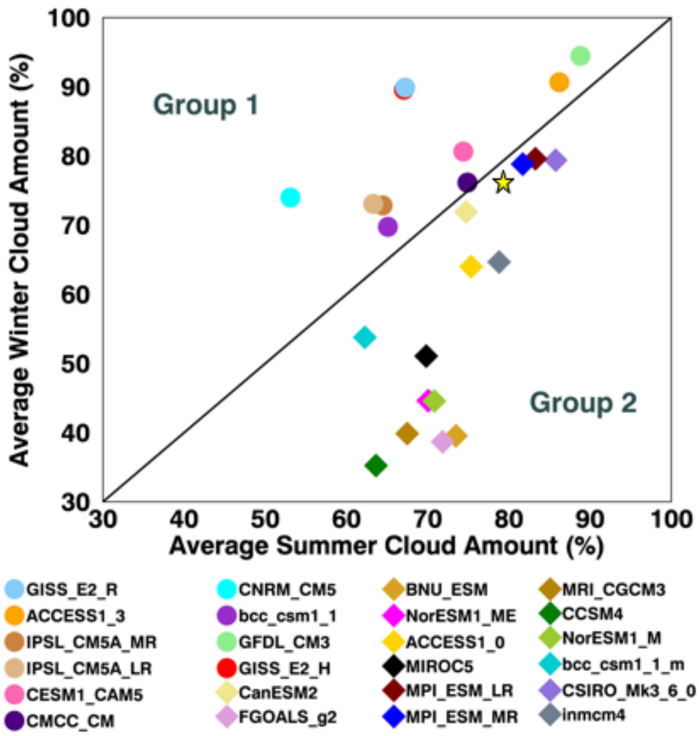

Figure 2: Average total cloud amount in winter (DJF) vs average summer (JJA). Models above the 1:1 line (maximum cloud amount in winter; circle symbols) are defined as Group 1 and those below the 1:1 line (maximum cloud amount in summer; square symbols) are Group 2. The yellow star represents C3M observations.

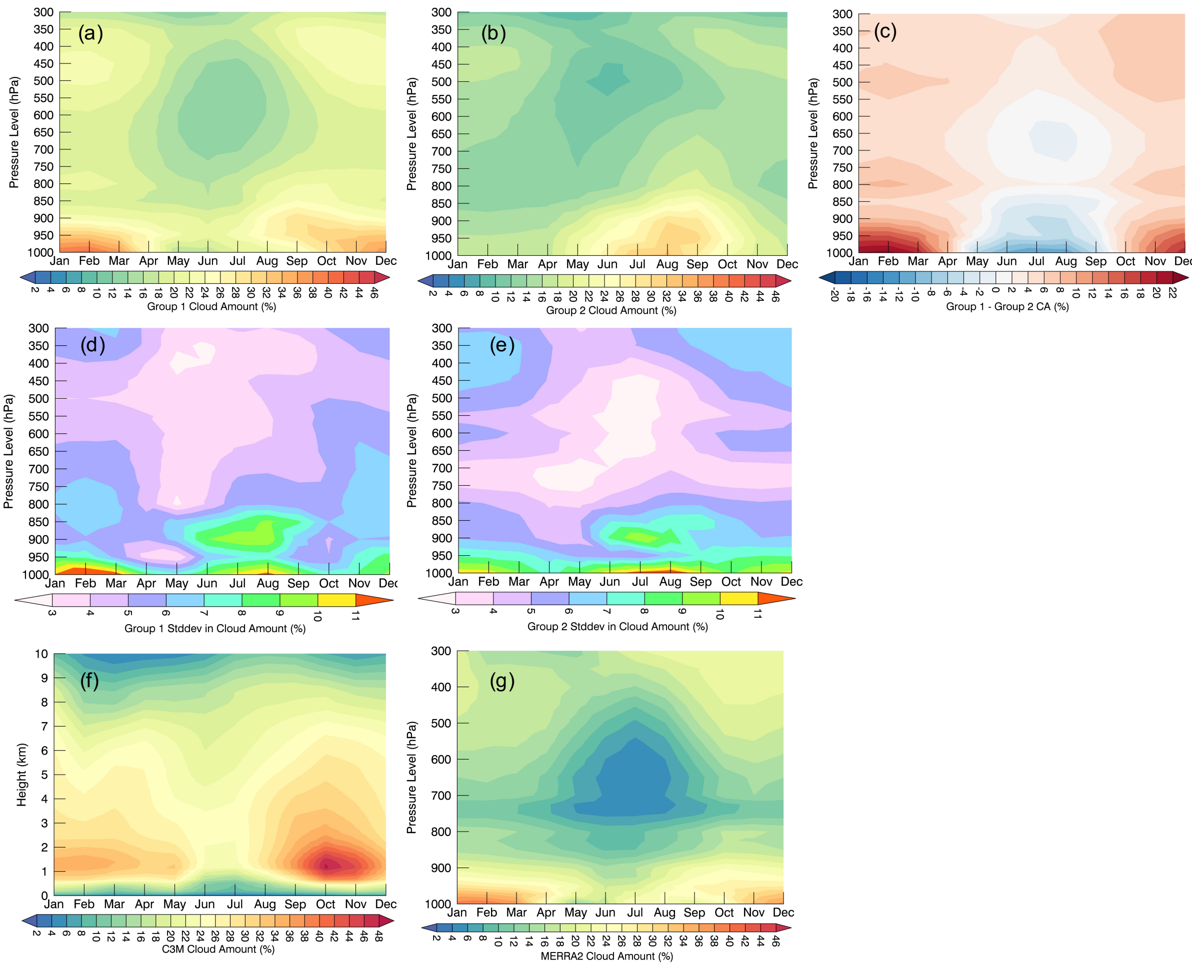

Figure 3: Vertically-resolved mean cloud amount annual cycle for (a) Group 1, (b) Group 2, and (c) Group 1 – Group 2. The vertically resolved standard deviation across the (d) Group 1 and (e) Group 2 members. Observational profiles of cloud amount are shown for (f) C3M and (g) MERRA-2.

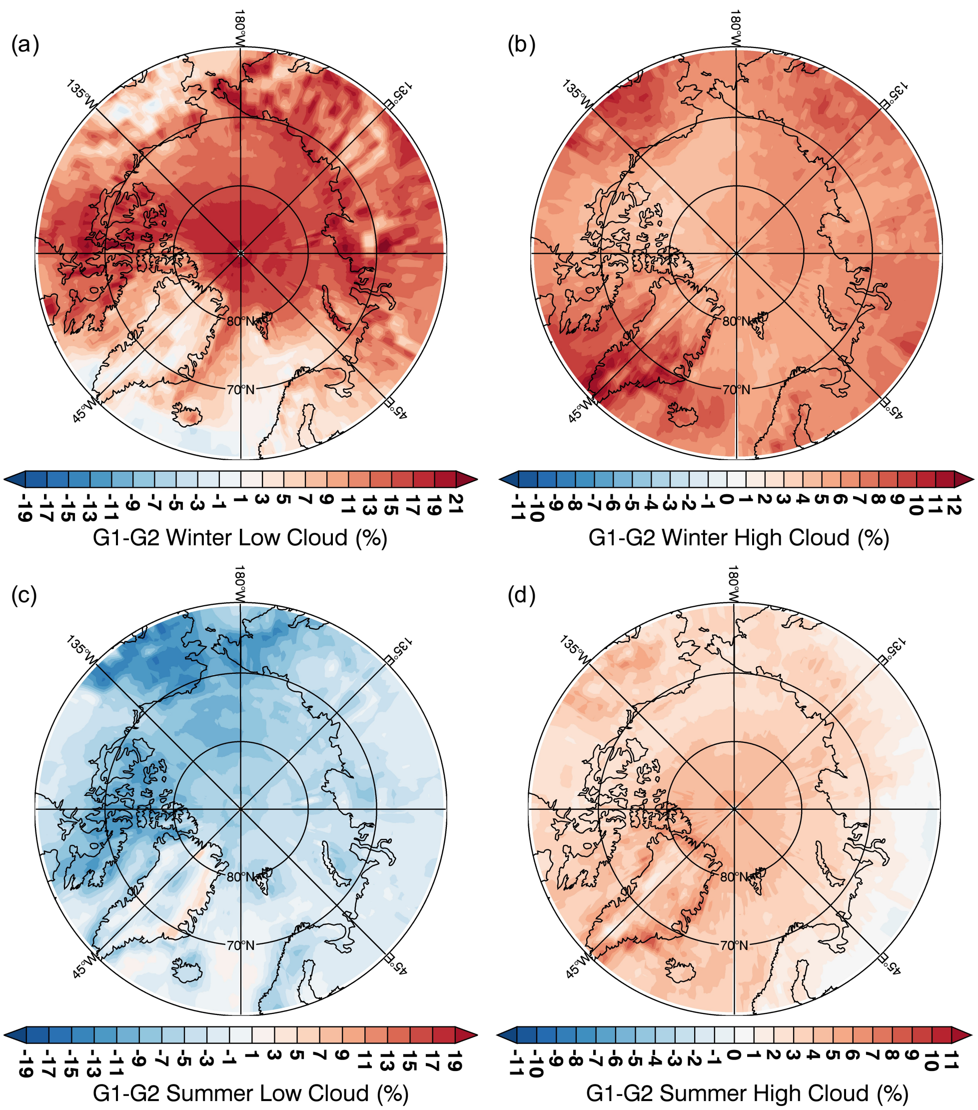

Figure 4: Spatial variations in Group 1 minus Group 2 cloud amount differences for (a) winter low clouds, (b) winter high clouds, (c) summer low clouds, and (d) summer high clouds.

Atmos. Chem. Phys. Discuss., https://doi.org/10.5194/acp-2018-1159
Manuscript under review for journal Atmos. Chem. Phys.
Discussion started: 21 December 2018

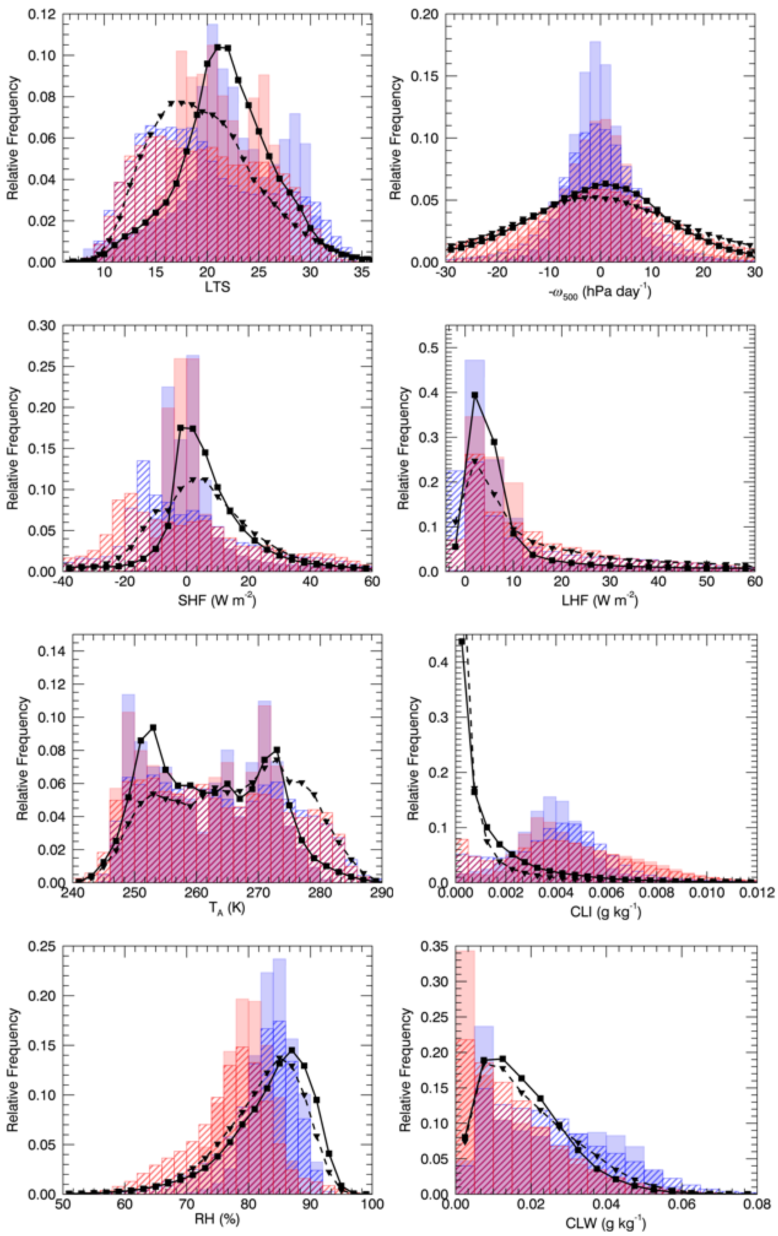

Figure 5: Probability distributions of (a) LTS, (b) $-\omega_{500}$, (c) low-level T_A, (d) CLI, (e) SHF, (f) LHF, (g) RH, and (h) CLW. Red shading denotes Group 1, blue denotes Group 2, solid fill represents ocean grid boxes, and cross-hatching represents land grid boxes. The solid black line shows MERRA-2 reanalysis values for ocean (square symbol) and land (triangle symbol). Distributions include all months of the year.

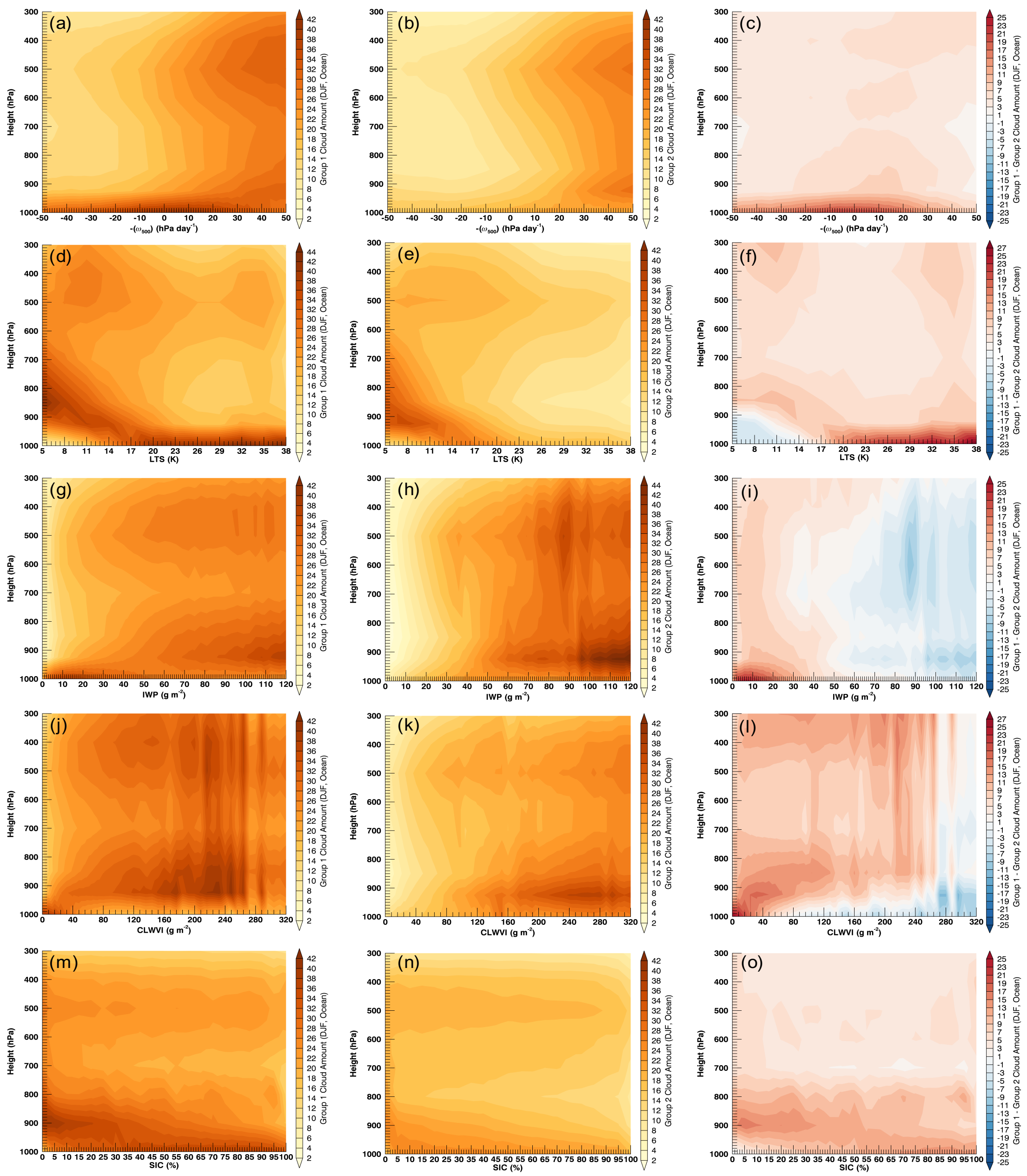

Figure 6: Vertically-resolved, DJF average cloud amount stratified by $-\omega_{500}$ for (a) Group 1, (b) Group 2, and (c) Group 1 minus Group 2, LTS for (d) Group 1, (e) Group 2, and (f) Group 1 minus Group 2, IWP for (g) Group 1, (h) Group 2, and (i) Group 1 minus Group 2, CLWVI for (j) Group 1, (k) Group 2, and (l) Group 1 minus Group 2, and SIC for (m) Group 1, (n) Group 2, and (o) Group 1 minus Group 2. All panels are for ocean.

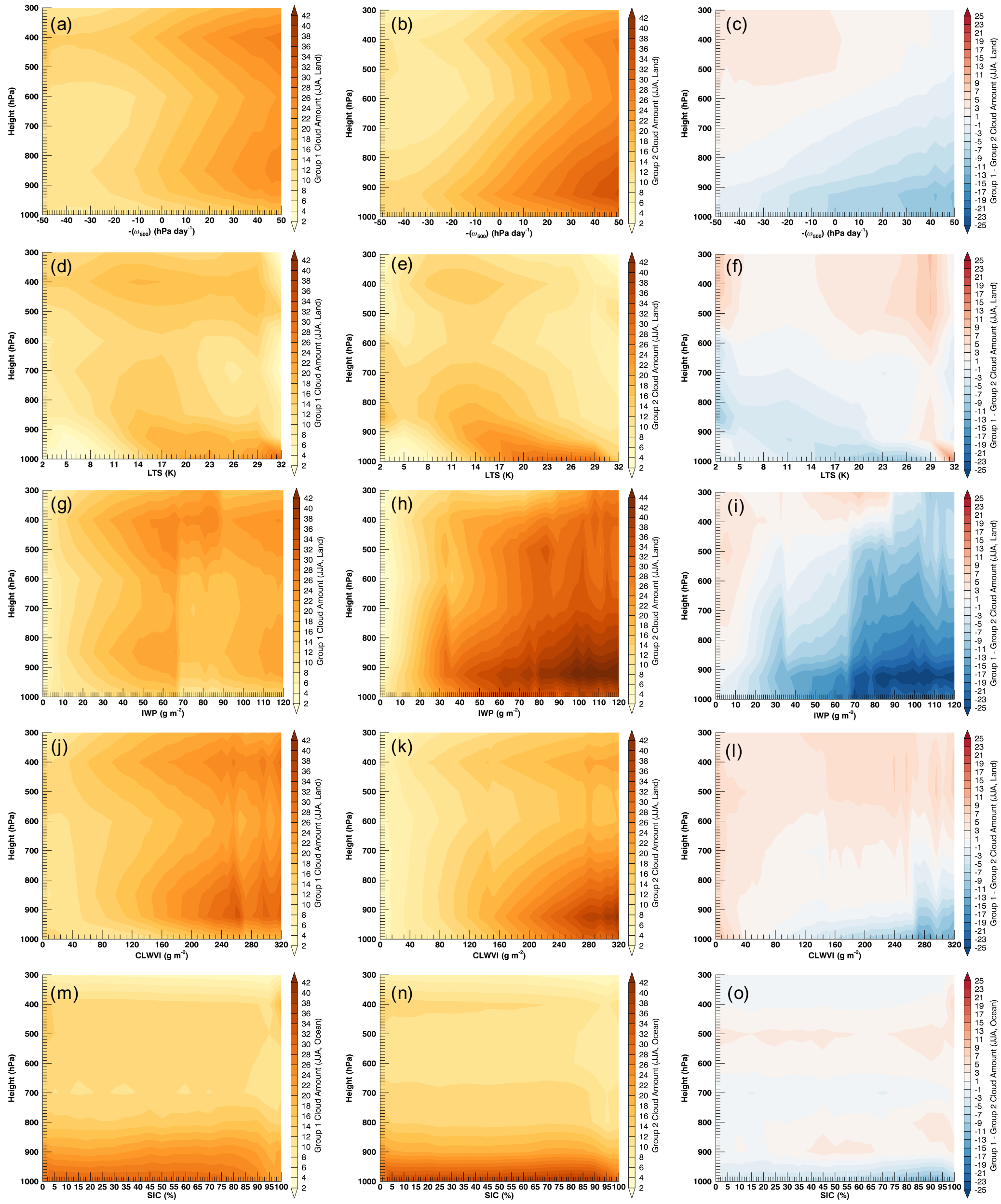

Figure 7: Vertically-resolved, JJA cloud amount stratified by $-\omega_{500}$ for (a) Group 1, (b) Group 2, and (c) Group 1 minus Group 2, LTS for (d) Group 1, (e) Group 2, and (f) Group 1 minus Group 2, IWP for (g) Group 1, (h) Group 2, and (i) Group 1 minus Group 2, CLWVI for (j) Group 1, (k) Group 2, and (l) Group 1 minus Group 2, and SIC for (m) Group 1, (n) Group 2, and (o) Group 1 minus Group 2. All panels are over land except for SIC.

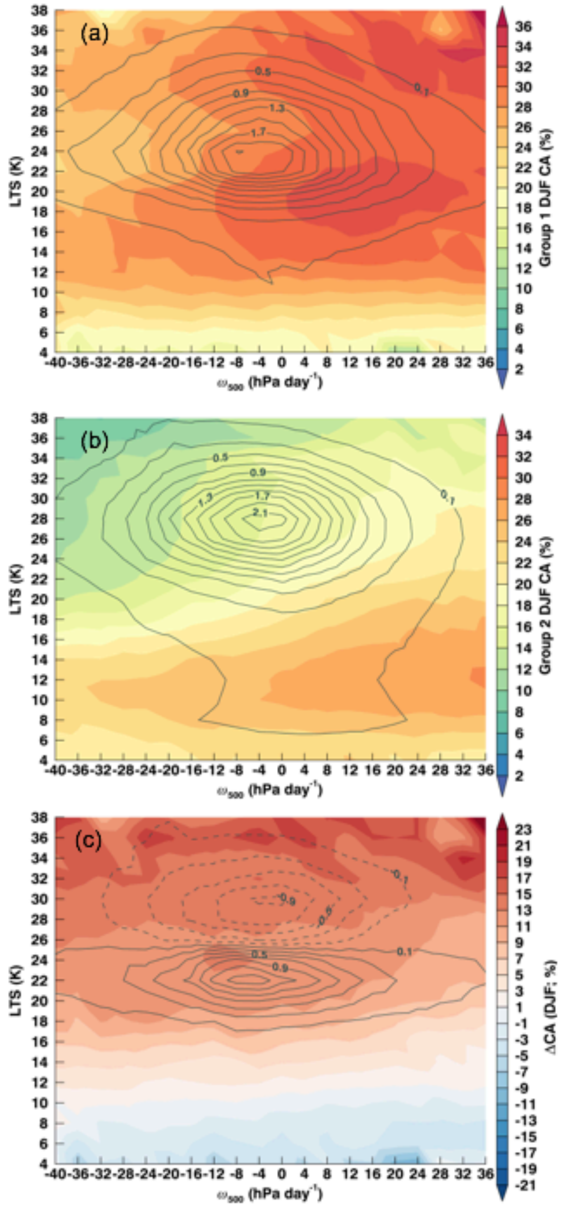

Figure 8: Contours of average low cloud amount for DJF in the LTS and $-\omega_{500}$ joint distribution for (a) Group 1, (b) Group 2, and (c) Group 1 minus Group 2. The frequency of occurrence each LTS and $-\omega_{500}$ bin is contoured in solid black with an interval of 0.2%.

Atmos. Chem. Phys. Discuss., https://doi.org/10.5194/acp-2018-1159
Manuscript under review for journal Atmos. Chem. Phys.
Discussion started: 21 December 2018

Atmospheric Chemistry and Physics
Discussions
Open Access

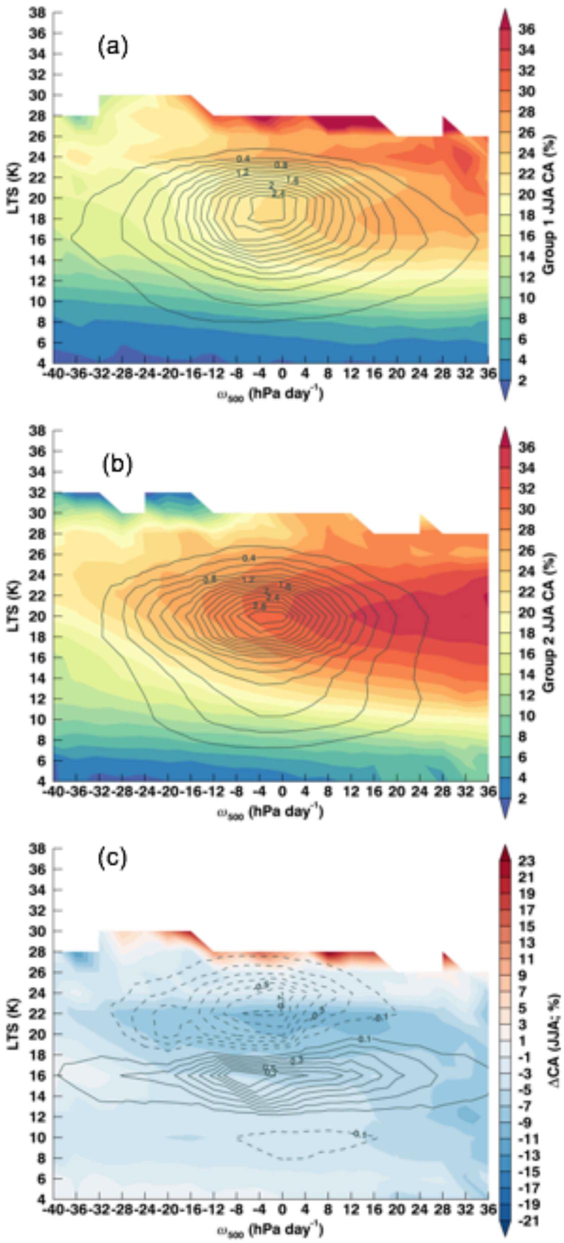

Figure 9: Contours of average low cloud amount for JJA in the LTS and $-\omega_{500}$ joint distribution for (a) Group 1, (b) Group 2, and (c) Group 1 minus Group 2. The frequency of occurrence each LTS and $-\omega_{500}$ bin is contoured in solid black with an interval of 0.2%.

Atmos. Chem. Phys. Discuss., https://doi.org/10.5194/acp-2018-1159
Manuscript under review for journal Atmos. Chem. Phys.
Discussion started: 21 December 2018

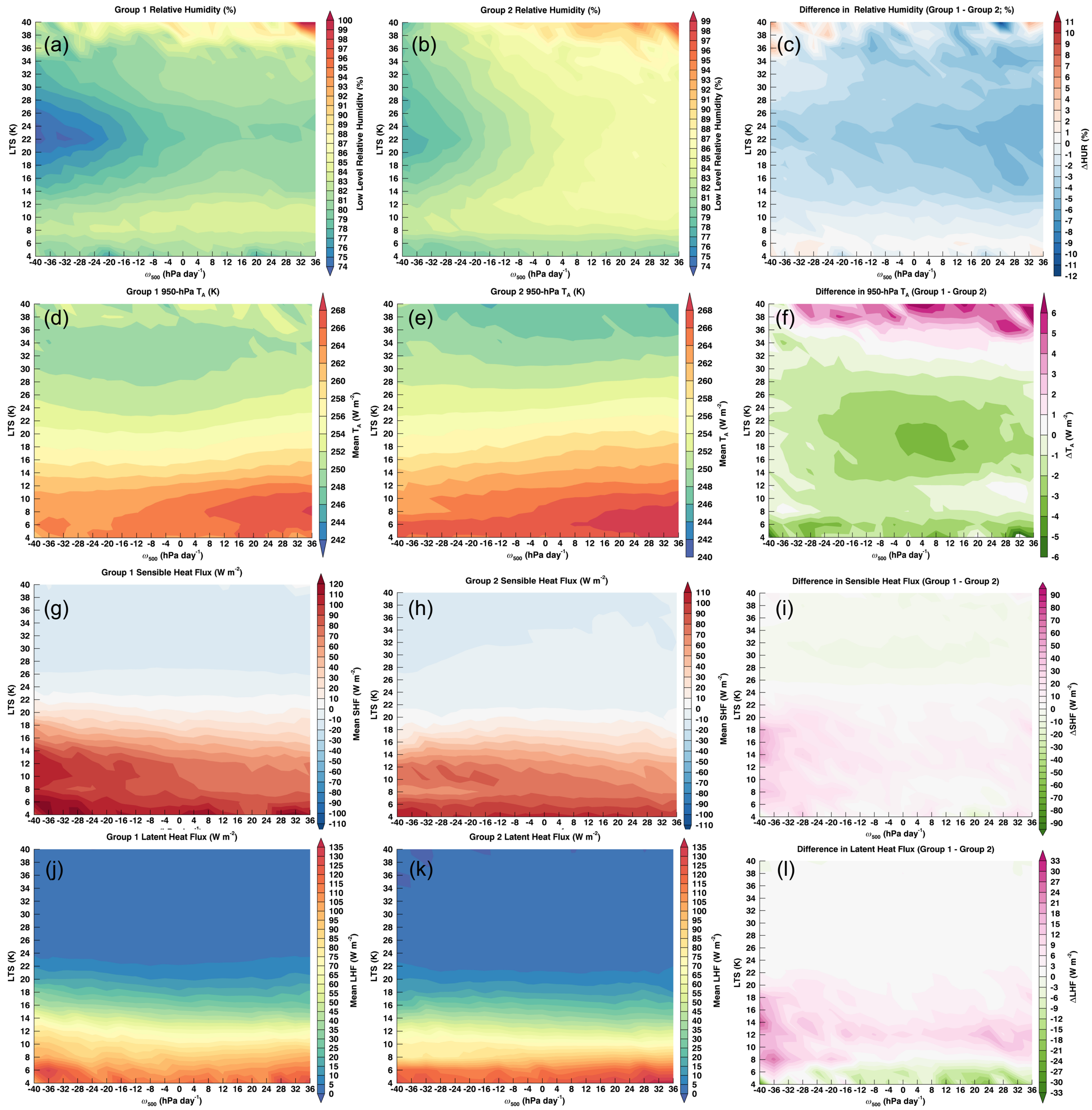

Figure 10: Contours of DJF atmospheric and surface conditions in the LTS and -ω_{500} joint distribution for (left column) Group 1, (middle column) Group 2, and (right column) Group 1 minus Group 2 for (a-c) RH, (d-f) T_A at 950hPa, (g-l) SHF, and (j-l) LHF.

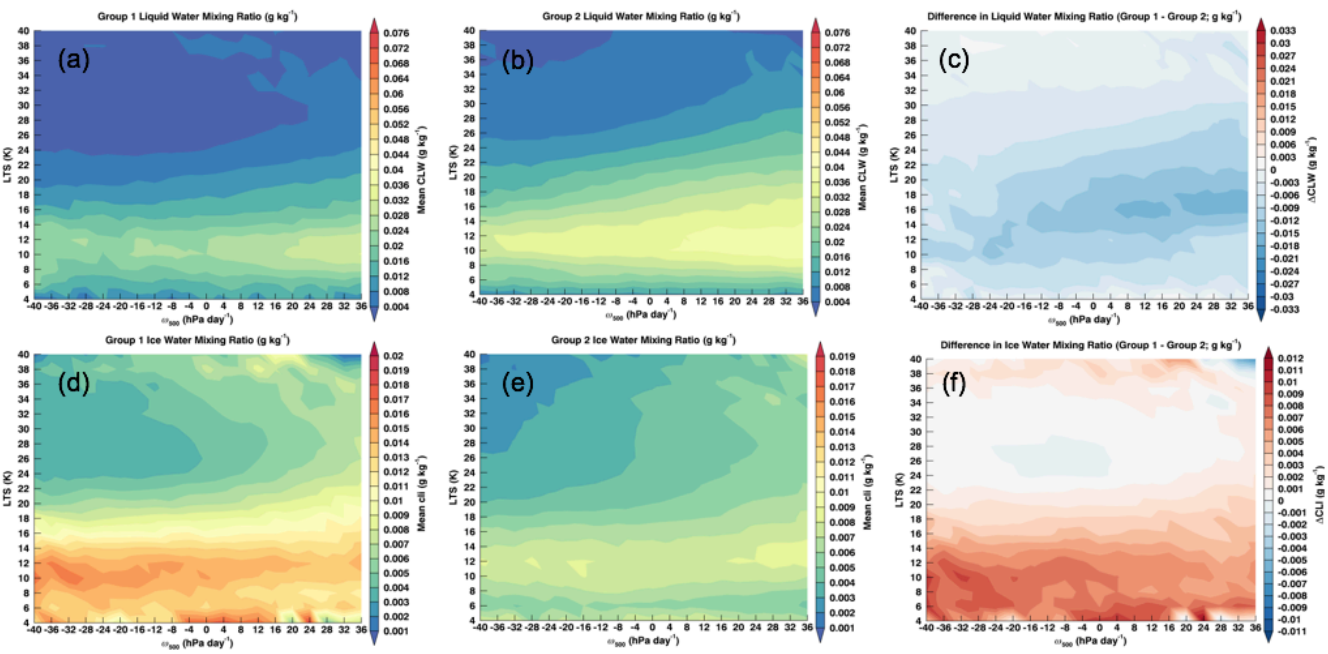

Figure 11: Contours of DJF low cloud CLW for (a) Group 1, (b) Group 2, and (c) Group 1 minus Group 2 and CLI (d) Group 1, (e) Group 2, and (f) Group 1 minus Group 2.

Atmos. Chem. Phys. Discuss., https://doi.org/10.5194/acp-2018-1159
Manuscript under review for journal Atmos. Chem. Phys.
Discussion started: 21 December 2018

Atmospheric Chemistry and Physics
Open Access
Discussions

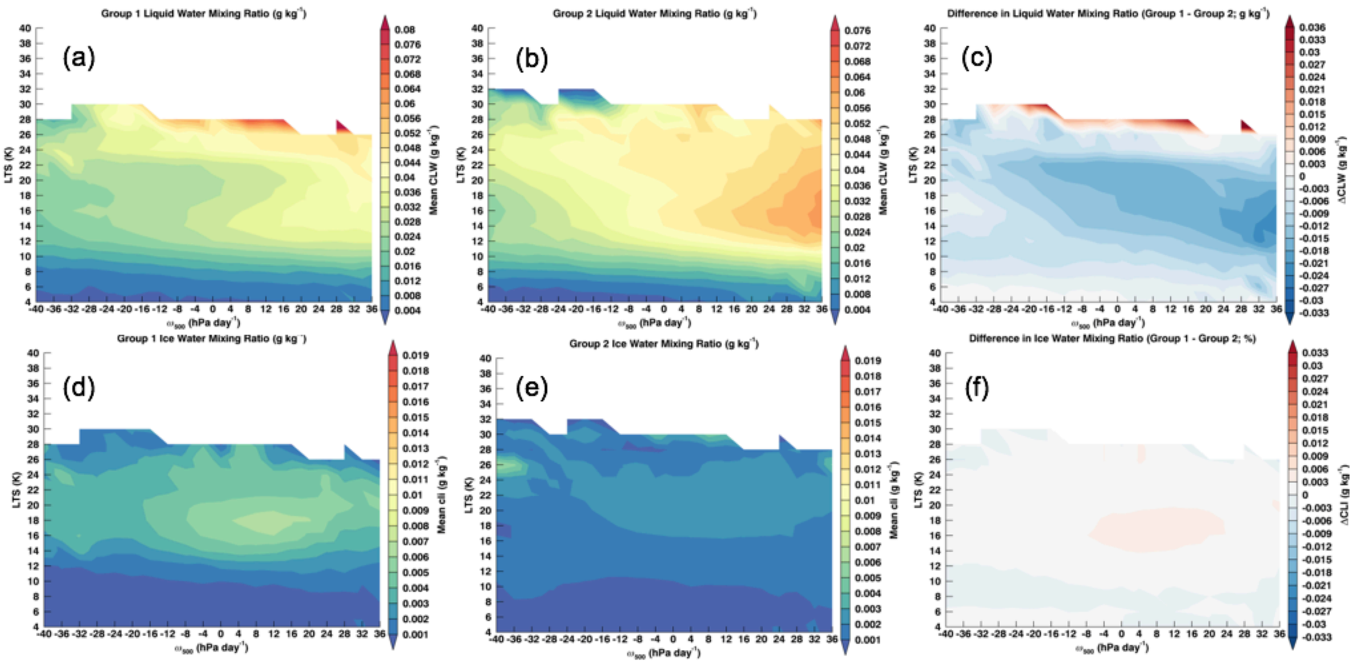

Figure 12: Contours of JJA low cloud CLW for (a) Group 1, (b) Group 2, and (c) Group 1 minus Group 2 and CLI (d) Group 1, (e) Group 2, and (f) Group 1 minus Group 2.

Atmos. Chem. Phys. Discuss., https://doi.org/10.5194/acp-2018-1159
Manuscript under review for journal Atmos. Chem. Phys.
Discussion started: 21 December 2018

Atmospheric Chemistry and Physics Discussions
Open Access

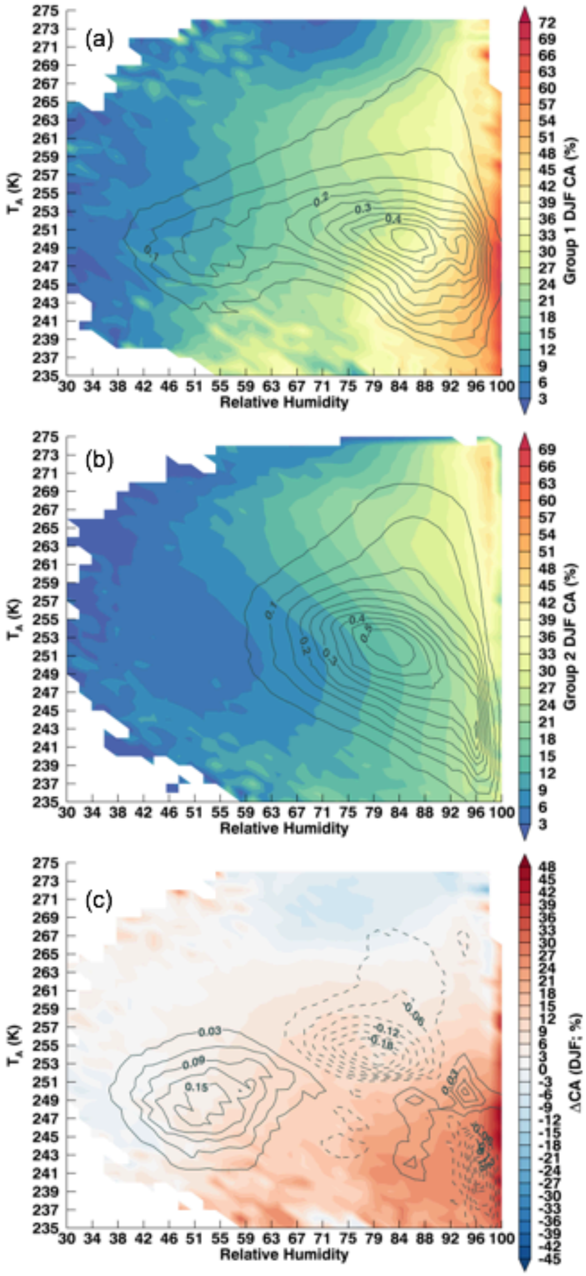

Figure 13: Contours of average low cloud amount for DJF the T_A-RH joint distribution for (a) Group 1, (b) Group 2, and (c) Group 1 minus Group 2. The frequency of occurrence of each T_A-RH bins is contoured in solid black with an interval of 0.2%.

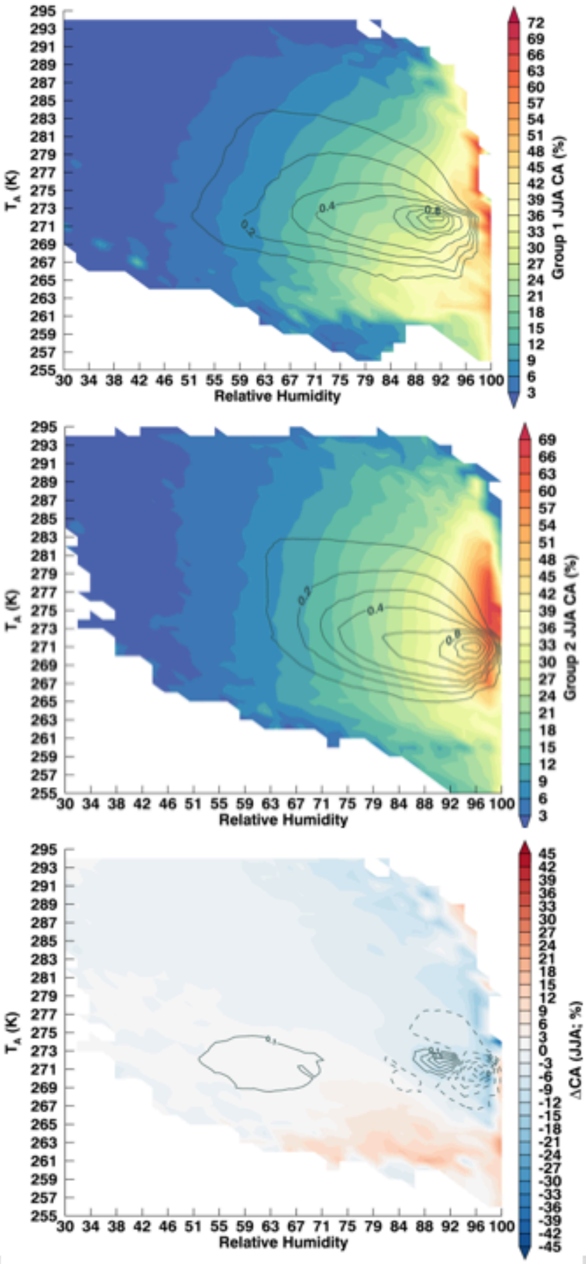

Figure 14: Contours of average low cloud amount for JJA the T_A-RH joint distribution for (a) Group 1, (b) Group 2, and (c) Group 1 minus Group 2. The frequency of occurrence of each T_A-RH bin is contoured in solid black with an interval of 0.2%.